Tbx1 has a dual role in the morphogenesis of the cardiac outflow tract

Huansheng Xu[1,3], Masae Morishima[3], John N. Wylie[6,7], Robert J. Schwartz[1,2,5], Benoit G. Bruneau[6,7], Elizabeth A. Lindsay[1,2,3] and Antonio Baldini[1,2,3,4,*]

[1]Program in Cardiovascular Sciences, Baylor College of Medicine, Houston, TX 77030, USA
[2]Center for Cardiovascular Development, Baylor College of Medicine, Houston, TX 77030, USA
[3]Departments of Pediatrics (Cardiology), Baylor College of Medicine, Houston, TX 77030, USA
[4]Molecular and Human Genetics, Baylor College of Medicine, Houston, TX 77030, USA
[5]Molecular and Cellular Biology, Baylor College of Medicine, Houston, TX 77030, USA
[6]Cardiovascular Research and Developmental Biology, The Hospital for Sick Children, University of Toronto, Toronto M5G 1X8, Canada
[7]Department of Molecular and Medical Genetics, University of Toronto, Toronto M5G 1X8, Canada
*Author for correspondence (e-mail: baldini@bcm.tmc.edu)

Accepted 17 March 2004

Development 131, 3217-3227
Published by The Company of Biologists 2004
doi:10.1242/dev.01174

Summary

Dysmorphogenesis of the cardiac outflow tract (OFT) causes many congenital heart defects, including those associated with DiGeorge syndrome. Genetic manipulation in the mouse and mutational analysis in patients have shown that Tbx1, a T-box transcription factor, has a key role in the pathogenesis of this syndrome. Here, we have dissected Tbx1 function during OFT development using genetically modified mice and tissue-specific deletion, and have defined a dual role for this protein in OFT morphogenesis. We show that Tbx1 regulates cell contribution to the OFT by supporting cell proliferation in the secondary heart field, a source of cells fated to the OFT. This process might be regulated in part by *Fgf10*, which we show for the first time to be a direct target of Tbx1 in vitro. We also show that *Tbx1* expression is required in cells expressing *Nkx2.5* for the formation of the aorto-pulmonary septum, which divides the aorta from the main pulmonary artery. These results explain why aortic arch patterning defects and OFT defects can occur independently in individuals with DiGeorge syndrome. Furthermore, our data link, for the first time, the function of the secondary heart field to congenital heart disease.

Key words: Tbx1, Mouse, Outflow tract, DiGeorge syndrome

Introduction

The cardiac outflow tract (OFT) forms as a simple vascular conduit that connects the embryonic right ventricle to the aortic sac, which is the site of confluence of the pharyngeal arch arteries. The embryonic OFT, which is divided into conal (proximal to the heart) and truncal (distal) segments, is soon lined by myocardial cells derived from migrating mesodermal cells. The myocardial layer of the embryonic OFT contracts and functions as a primitive valve. Septation separates the OFT into two channels, which direct the blood flow towards the aortic (systemic) and pulmonary circulation, and divides the primitive truncal valve into the aortic and pulmonary valves. Whereas the heart myocardium derives from lateral plate mesoderm precursors (the primary heart field), the OFT myocardium derives from the splanchnic mesoderm located caudal to the pharynx (the secondary heart field, or SHF) (Kelly et al., 2001; Mjaatvedt et al., 2001; Waldo et al., 2001). The molecular mechanisms underlying induction and differentiation of myocardial precursors in the SHF are hypothesized to be similar to those of the primary heart field (Waldo et al., 2001), but the genetics of SHF function and the phenotypic consequences of SHF malfunction are uncertain. Neural crest-derived cells are also required for OFT septation and make up most of the aorto-pulmonary (AP) septum, a structure that originates from the dorsal wall of the aortic sac (Jiang et al., 2000; Kirby and Waldo, 1995; Li et al., 2000). Severe developmental defects of the OFT are tolerated during embryogenesis, provided that they do not compromise patency, but are lethal in post-natal life, when the pulmonary circulation is required for blood oxygenation. OFT developmental defects account for a high proportion of congenital heart disease cases and, consequently, are an important cause of morbidity and mortality in children.

Chromosome 22q11.2 deletion (*del22q11*) causes most cases of DiGeorge syndrome (DGS), velocardiofacial syndrome, and conotruncal anomaly face, and it is one of the most common genetic causes of OFT and aortic arch defects. Modeling *del22q11* in mice (Jerome and Papaioannou, 2001; Lindsay et al., 1999; Lindsay et al., 2001; Merscher et al., 2001) and mutational analysis in human patients (Yagi et al., 2003), have led to the identification of *Tbx1* as the major player in these syndromes. Tbx1 is required for segmentation of the embryonic pharynx, for the formation of the caudal pharyngeal arches and arch arteries, and for growth, alignment and septation of the OFT in mice. Because of the complexity of the mutant phenotype, and the close developmental relationship between the pharyngeal apparatus and OFT, it has not been possible to establish whether Tbx1 has a specific role in OFT morphogenesis. Here we have addressed this issue using different genetic approaches in the mouse and we show that even in the presence of severe developmental abnormalities of the pharynx, the severity of the OFT phenotype can be ameliorated by a low level of *Tbx1* expression. Conversely, conditional ablation of *Tbx1* in the *Nkx2.5* domain causes a mild pharyngeal phenotype, but it recapitulates the severe OFT phenotype observed in *Tbx1*$^{-/-}$ embryos. Analysis of conditional mutants supports a dual role of *Tbx1* in OFT development, one in morphogenesis of the AP septum, and one in cell proliferation in the SHF region. Reduced cell proliferation in the SHF is associated with reduced cell contribution to the OFT and, consequently, reduced number of muscle cells.

Our data provide an explanation as to why OFT defects may occur independently from other pharyngeal or aortic arch patterning defects in patients with *del22q11*. We propose that the separation of the aorta and pulmonary arteries requires Tbx1 in the pharyngeal endoderm, whereas proper OFT alignment and truncal valve septation requires Tbx1 function in the SHF.

Materials and Methods

Mouse mutants and breeding

The following mouse lines have been described previously: Tie2-Cre (Kisanuki et al., 2001), αMHC-Cre (Agah et al., 1997), R26R (Soriano, 1999), *Tbx1*$^{+/-}$ (Lindsay et al., 2001), *Df1*/+ (Lindsay et al., 1999), *Nkx2.5*$^{Cre/+}$ (Moses et al., 2001). Mice were genotyped using PCR as described in the original reports. The generation of the new lines *Tbx1*$^{neo/+}$, *Tbx1*$^{flox/+}$, and *Tbx1*$^{mcm/+}$ is described below. To induce nuclear translocation of the MerCreMer fusion protein encoded by the *Tbx1*^{mcm} allele, pregnant mice were injected daily with Tamoxifen (30 mg/kg body weight) starting from E5.5. Consistent with literature data (Hayashi and McMahon, 2002), we observed that this dosage causes some embryo lethality, however, we did not observe cardiovascular defects in surviving wild-type embryos, and the expression of *Tbx1* (as tested by the *lacZ* knock-in reporter allele) was not affected by the Tamoxifen treatment (not shown).

Cell fate mapping in *Tbx1* homozygous mutant background was performed in *Df1*/*Tbx1*^{mcm};R26R embryos. The *Df1* deletion, which includes the *Tbx1* gene, was used as the *Tbx1* null allele because our *Tbx1*$^{+/-}$ allele includes a *lacZ* reporter gene that would have confounded the analysis. *Df1*/*Tbx1*$^{-}$ and *Tbx1*$^{-/-}$ have identical phenotype (Vitelli et al., 2002b). All mouse lines were crossed into a C57BL/6 background in the experiments described. All embryos (up to E12.5) were staged by counting the number of somites.

Generation of new mouse lines

The alleles *Tbx1*^{neo}, *Tbx1*^{mcm} were generated by homologous recombination in AB2.2 ES cells, as shown in Fig. 1A and Fig. 2A. The allele *Tbx1*^{flox} was generated by transfecting a Cre recombinase expression vector in *Tbx1*$^{neo/+}$ ES cells. ES cells were injected into C57Bl6 blastocysts and chimeric mice were crossed with C57BL/6 mice to obtain germ line transmission of the mutant alleles. Cre-induced recombination of the floxed allele causes the excision of exon 5 and generation of the *Tbx1*$^{\Delta E5}$ allele (Fig. 1B). This deletion is predicted to cause loss of function because exon 5 encodes part of the conserved T-box domain, and because splicing between exons 4 and 6 in the mutant allele generates a frame shift from codon 169, and a stop codon after 86 codons. We could not detect exon 5 skipping in the wild-type allele using reverse-transcription polymerase chain reaction (RT-PCR) on RNA from E10.5 embryos.

The *Tbx1*^{neo} allele was genotyped with primer pair Tbx1-neo_F: GGCCCTGCCTAACTCAGATT and Tbx1-neo_R: TGGCCCATG-TTCCTTTTATT. The *Tbx1*^{flox} allele was genotyped with the primer pair Tbx1-flox_F: CGACCCTTCTCTGGCTTATG and Tbx1-flox_R: AAAGACTCCTGCCCTTTTCC. The *Tbx1*^{mcm} allele was genotyped with the primer pair Tbx1-mcm_F: GCTCCACTTCAGCACATTCC and Tbx1-mcm_R: CATAAGCCAGAGAAGGGTCG.

RT-PCR

Total RNA was extracted from whole embryos at E10.5 using Trizol (Invitrogen). The concentration of RNA samples was measured using a spectrophotometer, and the concentration of all samples was adjusted to 100 ng/μl. The reverse transcription was followed by 30 cycles of PCR amplification. The location of the primers is indicated in Fig. 1A, the sequences are TTTGTGCCCGTAGATGACAA (forward primer) and AATCGGGGCTGATATCTGTG (reverse primer).

Analysis of chimeras

The generation of *Tbx1*$^{-/-}$ mouse ES cells has been described (Vitelli et al., 2003). *Tbx1*$^{-/-}$ and *Tbx1*$^{+/-}$ (Lindsay et al., 2001) ES cells were injected into wild-type C57BL/6 blastocysts and transferred into pseudopregnant CD1 females. Chimeric embryos were harvested at E10.5 and were stained with X-gal prior to ethanol fixation and embedding in paraffin. Histological sections (10 μm) were counterstained with Nuclear Fast Red.

Histology, X-gal staining and immunohistochemistry

To visualize β-gal activity, we stained paraformaldehyde-fixed embryos using the X-gal substrate, according to standard procedures. Stained embryos were photographed as wholemounts and then embedded in paraffin and cut in 10 μm histological sections. Sections were counterstained with Nuclear Fast Red. Muscle cells were identified by immunohistochemistry using an anti-α-smooth muscle actin (sma) monoclonal antibody (Clone 1A4, Sigma). Cell proliferation was assessed using a BrdU assay. Briefly, pregnant females were injected with 5 mg/100 g body weight of BrdU and sacrificed 1 hour after injection to harvest embryos. Embryos were fixed in ethanol, embedded in paraffin and cut in 7 μm sections. BrdU incorporation was detected on histological sections using an anti-BrdU monoclonal antibody (Clone # 85-2C8, Novacastra). The anti-neurofilament-M (165kD) monoclonal antibody 2H3 was developed by T. M. Jessell and J. Dodd and was obtained from the Developmental Studies Hybridoma Bank, University of Iowa.

RNA in situ hybridization

RNA in situ hybridization experiments, with radioactive or non-radioactive probes, were performed on sectioned or wholemount embryos, respectively, according to published protocols (Albrecht et al., 1997). Labeled probes (sense and antisense) were prepared by reverse transcription of DNA clones in the presence of digoxigenin-conjugated UTP (Roche) or ^{35}S-UTP (ICN). A *Tbx1* probe (Chapman et al., 1996) was obtained from V. Papaioannou. *Crabp1* transcripts were detected using the probe described (Giguere et al., 1990).

Luciferase assay

A mouse *Tbx1* cDNA (Lindsay et al., 2001) (Accession # AF326960) was fused with a c-myc tag and cloned into the pCDNA3.1 expression vector. The *Fgf10Luc* and *Fgf10MutLuc* constructs, and the luciferase assay procedure have been described (Agarwal et al., 2003). Constructs were transfected in COS-7 cells and data were normalized to a co-transfected β-Gal expression vector. Experiments were performed in duplicate and repeated three times.

Results

Outflow tract development is Tbx1-dosage dependent

Tbx1$^{-/-}$ animals have severe OFT abnormalities including complete lack of septation and abnormal alignment of the

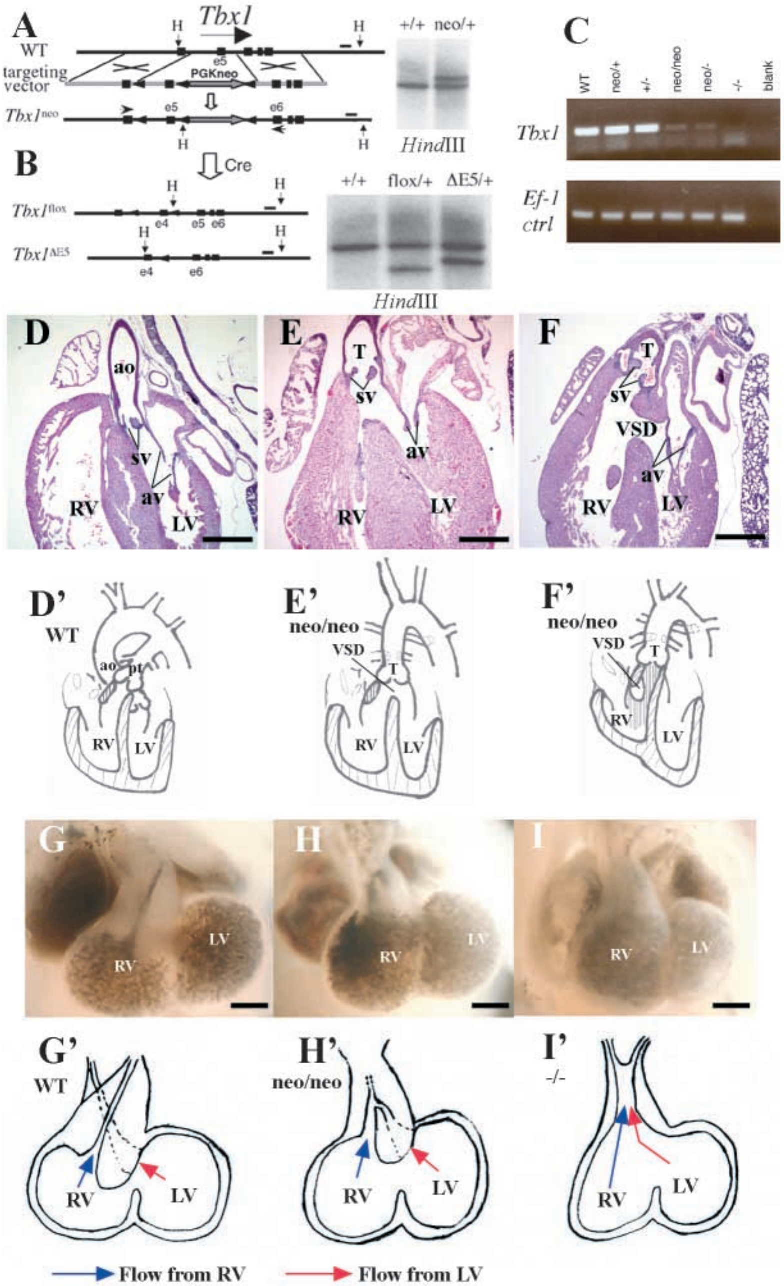

Fig. 1. Generation and phenotypic analysis of a hypomorphic *Tbx1* mutant. (A) Gene targeting strategy used to generate the *Tbx1*^{neo} allele. (B) Generation of the loxP-flanked (flox) *Tbx1*^{flox} allele. (C) RT-PCR shows low amount of *Tbx1* transcript expressed by the *Tbx1*^{neo} allele. The RNA was extracted from whole E10.5 embryos. (D-F) Alignment of the OFT in E18.5 embryos; in a *Tbx1*$^{+/+}$ embryo (D) the aorta (ao) communicates with the left ventricle (LV), in a *Tbx1*$^{neo/neo}$ mutant (E) with correct alignment, the truncus (T) communicates with both left and right ventricles (RV). However, in the *Tbx1*$^{neo/neo}$ embryo shown in F, the truncus communicates only with the RV (as in *Tbx1*$^{-/-}$ embryos, not shown). (G-I) Intracardiac ink injection of E11.5 embryos shows normal OFT alignment in a *Tbx1*$^{+/+}$ embryo (G), lack of alignment in a *Tbx1*$^{-/-}$ embryo (I), and an intermediate phenotype in a *Tbx1*$^{neo/neo}$ embryo (H). av: atrioventricular valves; pt: pulmonary trunk; sv: semilunar valves; VSD: ventricular septum defect. Scale bars: 0.5 mm.

truncus arteriosus with the ventricles (Jerome and Papaioannou, 2001; Vitelli et al., 2002b). These abnormalities may be secondary to the severe defects of the pharyngeal apparatus associated with Tbx1 loss of function or may be because of a specific role of Tbx1 in OFT development. To begin addressing this issue, we have generated a new allelic series of the *Tbx1* gene, as shown in Fig. 1A,B. We tested in vivo whether a *Tbx1*^{neo} allele, which carries a PGKneo cassette inserted into intron 5, functions as a hypomorphic allele. *Tbx1*$^{neo/+}$ fetuses were examined at E18.5 (n=36) and 42% had the same aortic arch patterning defects observed in *Tbx1*$^{+/-}$ animals (not shown). We extracted RNA from *Tbx1*$^{neo/neo}$ and from *Tbx1*$^{neo/-}$ embryos and performed RT-PCR using primers on exons flanking the PGKneo cassette insertion (Fig. 1A). Results show that the *Tbx1*^{neo} allele transcribes a low amount of *Tbx1* RNA (Fig. 1C). *Tbx1*$^{neo/-}$ embryos were grossly indistinguishable from *Tbx1*$^{-/-}$ embryos, and show the same cardiovascular phenotype. However, none of the five *Tbx1*$^{neo/-}$ embryos examined at E18.5 had cleft palate, a defect observed in all the *Tbx1*$^{-/-}$ embryos examined in this genetic background (Vitelli et al., 2002a). Analysis of the cardiovascular phenotype revealed that out of 14 *Tbx1*$^{neo/neo}$ fetuses examined, eight had an alignment defect of the truncus identical to that observed in *Tbx1*$^{-/-}$ embryos (Fig. 1F,F′), whereas six had correct alignment (Fig. 1E,E′) as the truncus communicates directly with both ventricles and overrides a subvalvular ventricular septal defect (VSD). Improved OFT alignment was also evident at E11.5 (Fig. 1G-I). However, the pharyngeal phenotypes in *Tbx1*$^{neo/neo}$ and *Tbx1*$^{-/-}$ embryos were essentially identical at E10.5 (not shown). Thus the OFT phenotype resulting from loss of *Tbx1* function can be partially rescued even in the presence of severe pharyngeal abnormalities.

Tbx1 is not required in myocytes or endothelial cells of the OFT

Despite the severity of the OFT phenotype in *Tbx1*$^{-/-}$ mutants, *Tbx1* gene expression in the OFT is modest (Vitelli et al., 2002b). *Tbx1* is expressed in endothelial cells (from E11.5) and in a subpopulation of α-sma-positive cells of the outer wall of the OFT (Vitelli et al., 2002b). Endothelial cells in the conal OFT, transform into mesenchymal cells of the outflow ridges (van den Hoff et al., 1999), thus, these cells might be important for septation and valvulogenesis. Therefore, we asked whether *Tbx1* is required by endothelial cells for conal septation. To this end, we used mice carrying a *Tbx1* conditional, floxed allele, generated as shown in Fig. 1B. *Tbx1*$^{flox/flox}$ mice were viable and fertile, and were crossed with *Tbx1*$^{+/-}$;Tie2:Cre mice. Tie2:Cre transgenic mice express Cre in endothelial cells and their precursors (Kisanuki et al., 2001), including endothelial cells of the OFT that also express *Tbx1* (not shown). *Tbx1*$^{flox/-}$; Tie2:Cre fetuses were analyzed at E18.5 (n=8), but none presented with cardiovascular abnormalities other than aortic arch defects associated with *Tbx1* haploinsufficiency (not shown). Next, we asked whether *Tbx1* expressed in muscle cells of the OFT is required for OFT growth and morphogenesis. To this end, we crossed $Tbx1^{+/-}$; αMHC:Cre mice with $Tbx1^{flox/flox}$ mice. $Tbx1^{flox/-}$; αMHC:Cre fetuses at E18.5 (*n*=6) had normal cardiovascular phenotype, apart from the aortic arch abnormalities characteristic of *Tbx1* haploinsufficiency (not shown).

Tbx1 is expressed in precursors of OFT cells and its loss of function reduces cell contribution to the OFT

Because Tbx1 is not required in resident, differentiated OFT cells, we asked whether *Tbx1* may be expressed in progenitors of these cells. Therefore, we analyzed the fate of *Tbx1*-expressing cells by generating and establishing in mice an allele of *Tbx1*, named $Tbx1^{mcm}$, in which a Tamoxifen-inducible Cre construct (Sohal et al., 2001; Verrou et al., 1999) is driven by the endogenous regulatory elements of *Tbx1* (Fig. 2A). The insertion point of the Cre construct is identical to the one we used for a *lacZ* reporter construct shown to recapitulate the developmental expression of *Tbx1* (Lindsay et al., 2001; Vitelli et al., 2002b). We then crossed $Tbx1^{mcm/+}$ mice with the R26R reporter line (Soriano, 1999) to evaluate Cre-induced recombination. Because the Cre construct that we used encodes a Tamoxifen-inducible recombinase, $Tbx1^{mcm/+}$;R26R embryos from mothers that had not been injected with Tamoxifen showed no blue cells upon X-gal staining (*n*=13, not shown). The cell fate of *Tbx1*-expressing cells was studied using $Tbx1^{mcm/+}$;R26R embryos where the pregnant mothers had been treated with daily injections of Tamoxifen from E5.5. Hereafter we refer to these embryos, stained with X-gal, as *Tbx1*-tracing embryos. The staining intensity was variable but, overall, *Tbx1* tracing resulted in a pattern of X-gal staining that was very similar to *Tbx1* gene expression (Fig. 2B,C), at the stages tested (E9.5, E10.5 and E12.5), with two exceptions. First, the ectoderm lining the lateral aspect of the pharyngeal region showed extensive staining (Fig. 2C, red arrowheads), probably because of transient *Tbx1* expression in the ectoderm before E9.5 (E.A.L., unpublished). Second, in the OFT (Fig. 2E-J), *Tbx1* tracing showed extensive contribution to the myocardial wall and endothelium of the OFT, and some contribution to the myocardium of the right ventricle (Fig. 2F,H,J) (five embryos analyzed at E9.5, seven at E10.5, and four at E12.5). In contrast, *Tbx1* expression in the OFT was much more restricted (Fig. 2E,G,I), indicating that *Tbx1* is expressed transiently in a substantial number of progenitors of cells fated to the OFT. Contribution of *Tbx1*-traced cells was observed at all stages tested but was relatively low at E9.5 (earliest stage analyzed is 25 somite), suggesting that although this contribution must start before E9.5, it appears more substantial between E9.5 and E10.5.

Next, we asked whether Tbx1 function is required for the contribution of *Tbx1*-traced cells to the OFT. We performed cell fate mapping in a *Tbx1* null background and observed reduced number of *Tbx1*-traced cells in the OFT (Fig. 2D,L,M). However, this reduction could be attributed in part to the overall size reduction of the OFT in *Tbx1* null mutants. *Tbx1*-traced cells were observed in the SHF region of *Tbx1* homozygous mutant embryos (*n*=4) (Fig. 2M′ arrowhead, compare with *lacZ* knock-in K′ and cell fate mapping in heterozygous background, L′). Thus, *Tbx1* loss of function reduces but does not prevent the contribution of *Tbx1*-traced cells to the OFT and SHF.

Tbx1 is required in *Nkx2.5*-expressing cells

The data presented so far support the hypothesis that the primary role of *Tbx1* in OFT morphogenesis is performed in progenitors of cells contributing to the OFT. The induction of naïve mesodermal cells in the SHF to an OFT myocardial fate is thought to use a molecular circuitry similar to that used in the primary heart field (Waldo et al., 2001). Consistent with this view, *Nkx2.5* is expressed in the SHF (Kelly et al., 2001; Mjaatvedt et al., 2001; Waldo et al., 2001) and it is required for the development of the OFT (Lyons et al., 1995; Tanaka et al., 1999). The OFT of $Nkx2.5^{-/-}$ embryos is not canalized (Lyons et al., 1995; Tanaka et al., 1999) (M.M., unpublished), which is an earlier and more severe defect than that of $Tbx1^{-/-}$ animals. Hence, we hypothesize that Tbx1 function in OFT progenitors is downstream to Nkx2.5 function, and that deletion of *Tbx1* in cells expressing *Nkx2.5* is sufficient to recapitulate the OFT abnormalities found in $Tbx1^{-/-}$ mutants. To test this hypothesis, we crossed $Nkx2.5^{Cre/+}$ mice, which carry a Cre gene inserted into the *Nkx2.5* gene (Moses et al., 2001), with $Tbx1^{+/-}$ animals, and then crossed $Nkx2.5^{cre/+}$;$Tbx1^{+/-}$ mice with $Tbx1^{flox/flox}$ mice. The external appearance of E18.5 $Nkx2.5^{cre/+}$;$Tbx1^{flox/-}$ embryos (hereafter referred to as conditional mutants) was indistinguishable from that of normal littermates, in particular, they did not have the characteristic external ear defects or cleft palate observed in $Tbx1^{-/-}$ embryos (not shown). The thymus was clearly visible but small, with the lobes widely separated (Fig. 3A,B). The cardiovascular phenotype included truncus arteriosus of the same type as that seen in $Tbx1^{-/-}$ animals (complete lack of septation and a single four-leaflet truncal valve communicating exclusively with the right ventricle, and a large infundibular VSD) (Fig. 3C-E). The aortic arch phenotype differed from the $Tbx1^{-/-}$ phenotype because the 6th pharyngeal arch arteries (PAAs) formed, persisted and connected the outflow to the descending aorta (on the left) and to the right subclavian artery (on the right) (Fig. 3D′-E′). In contrast, in $Tbx1^{-/-}$ embryos the 3rd, 4th and 6th PAAs do not form (Vitelli et al., 2002b). Thus, conditional mutants recapitulate the OFT phenotype but not the aortic arch patterning phenotype of $Tbx1^{-/-}$ mutants, which is considerably milder in conditional mutants.

Because $Nkx2.5^{Cre}$ is a loss of function allele (Moses et al., 2001), and because Nkx2.5 has been shown to interact with another member of the T-box family of proteins, Tbx5 (Bruneau et al., 2001), we tested whether *Tbx1* and *Nkx2*.5 may interact genetically. However, double heterozygous $Nkx2.5^{Cre/+}$;$Tbx1^{+/-}$ embryos at E18.5 were viable (*n*=11) and presented with abnormalities attributable to haploinsufficiency of each gene (not shown), as both *Tbx1* (Jerome and Papaioannou, 2001; Lindsay et al., 2001; Merscher et al., 2001) and *Nkx2*.5 (Biben et al., 2000) are haploinsufficient. These results indicate that the OFT phenotype observed in conditional mutants is not because of genetic interaction between *Tbx1* and *Nkx2.5* but deletion of *Tbx1* in the *Nkx2.5* expression domain.

Conditional deletion of *Tbx1* causes ablation of the AP septum

Conditional mutants have normal 3rd and 6th PAAs but have

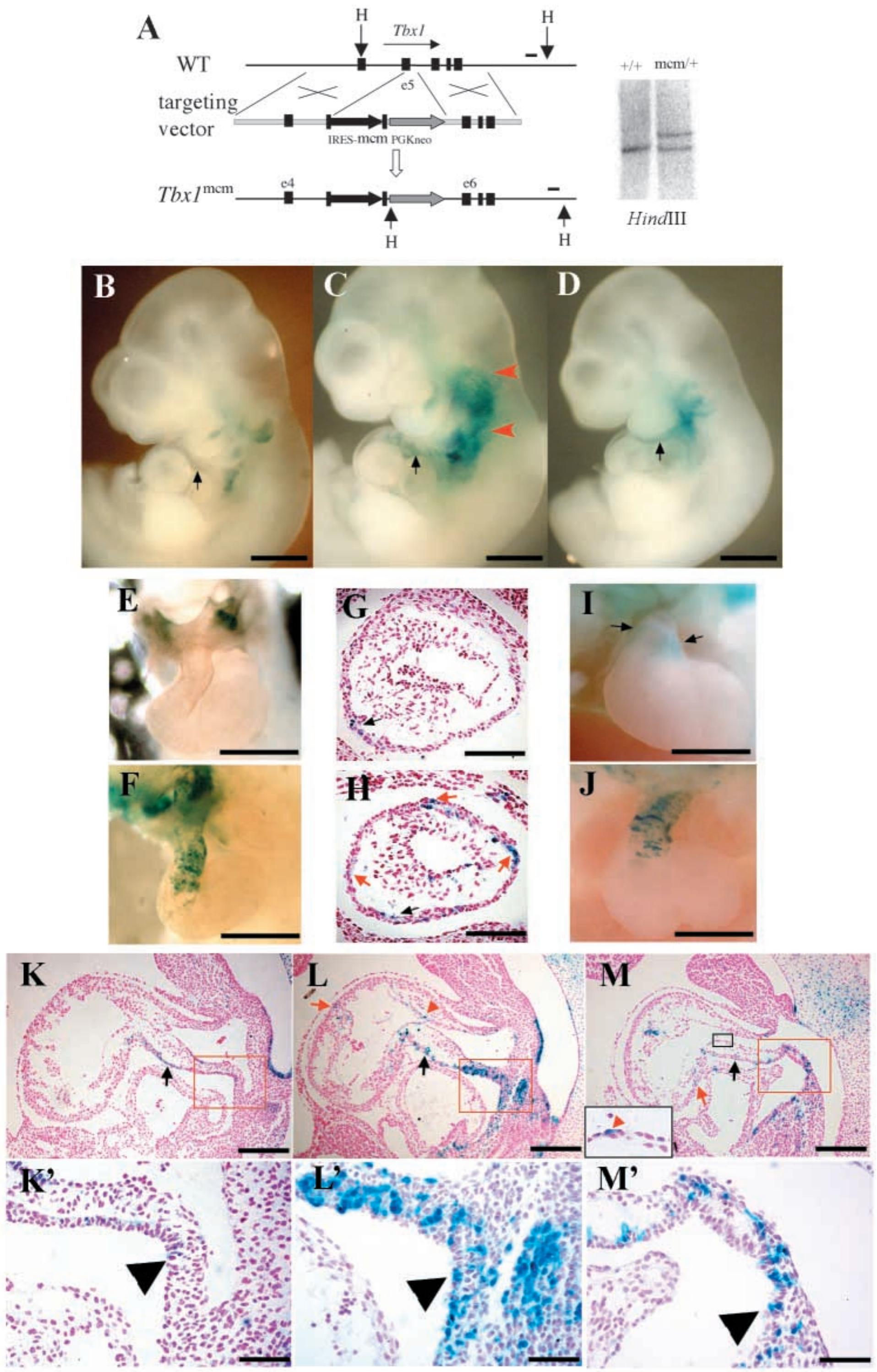

Fig. 2. Fate map of *Tbx1*-expressing cells. (A) The gene targeting strategy utilized to generate the *Tbx1*^{mcm} knock-in allele. (B) X-gal staining pattern generated by a *Tbx1-lacZ* knock-in allele (*Tbx1*$^{+/-}$) in an E10.5 embryo. (C) X-gal staining pattern in a *Tbx1*$^{mcm/+}$;R26R embryo at E10.5. (D) X-gal staining pattern in a *Df1/Tbx1*^{mcm};R26R embryo at E10.5 (*Tbx1* homozygous mutant background). Small arrows in B-D indicate the OFT, the red arrowheads in C point to a superficial, ectodermal domain. (E) Dissected heart from a *Tbx1*$^{+/-}$ (*lacZ* knock-in) E10.5 embryo, and, F, from a *Tbx1*$^{mcm/+}$;R26R E10.5 embryo. (G,H) Histological sections through the OFT at the same stage in *Tbx1*$^{+/-}$ (G) and *Tbx1*$^{mcm/+}$;R26R (F) embryos at E10.5. Black arrows show blue cells localized in similar position in the two mutants, red arrows indicate blue cells detected only by cell fate mapping. (I,J) X-gal staining pattern generated by a *Tbx1-lacZ* knock-in allele (*Tbx1*$^{+/-}$) in an E12.5 heart (I), compared with that in a *Tbx1*$^{mcm/+}$;R26R embryo (J) at the same stage. (K-M) Comparison of the *lacZ* knock-in X-gal staining pattern (K, 37 somites) with that obtained by cell fate mapping in a heterozygous (L, 39 somites) and homozygous (M, 36 somites) *Tbx1* mutant. The area in the black box in M is magnified (5×) in the inset at the bottom-left of M. K′-M′ show magnified details of panel K, L and M, respectively. Red arrowheads indicate endothelial cells, black arrows OFT myocytes, and black arrowheads SHF cells. Scale bars: 1 mm in B-D, E,F and I,J; 100 μm in G,H; 200 μm in K-M; 50 μm in K′-M′.

no 4th PAAs, as visualized by intracardiac ink injection (n=3) (Fig. 3F,G). This pattern is also seen in *Tbx1*$^{+/-}$ embryos, however, the distance between the 3rd and 6th PAAs is smaller than in wild-type or *Tbx1*$^{+/-}$ embryos, suggesting malformations of the 4th pharyngeal arch and aortic sac. Histological sections showed that the 4th pharyngeal arches of conditional mutants were small and the 4th PAAs were very hypoplastic or undetectable (Fig. 4A′,B′). Consistent with hypoplasia of the 4th pharyngeal arch, we observed a reduced number of neural crest-derived cells migrating through the 4th arch, but a normal pattern in the 3rd and 6th arches of conditional mutants, as tested by *Crabp1* in situ hybridization (Fig. 4C-F). Immunohistochemistry with an anti-neurofilament M antibody showed the presence of an apparently normal vagus nerve bundle in the 4th arch, suggesting normal differentiation of neural crest-derived cells in this arch (Fig. 4A,A′,B,B′).

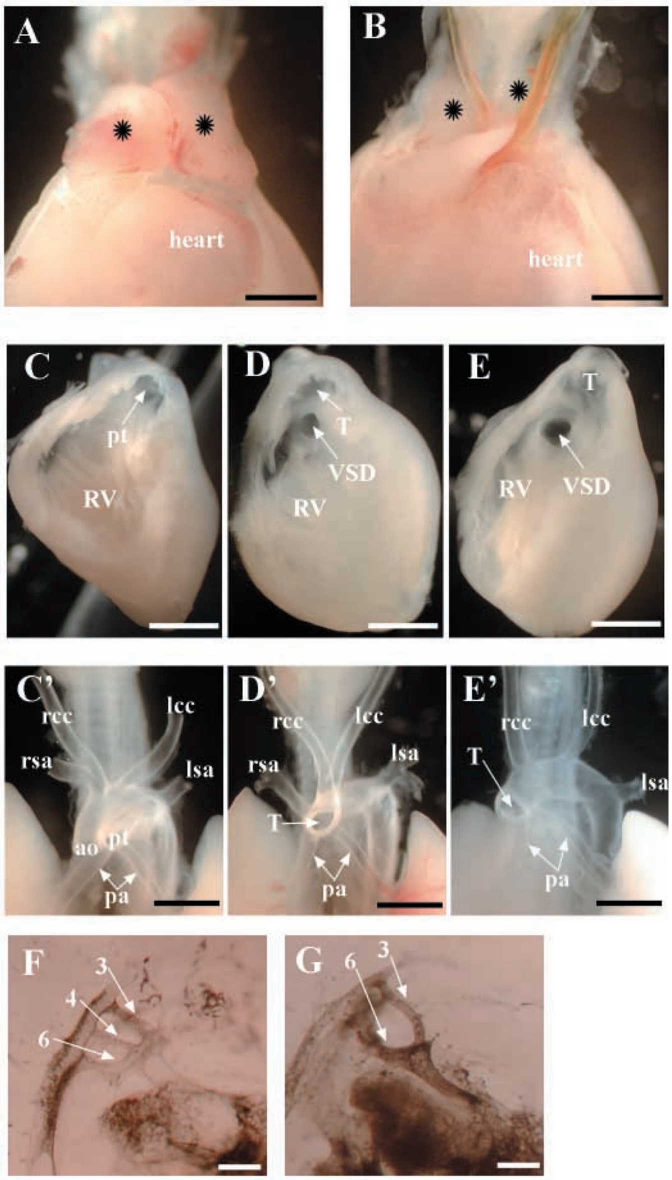

Fig. 3. Phenotype of conditional mutants *Nkx2.5*$^{Cre/+}$;*Tbx1*$^{flox/–}$. (A,B) Thymic hypoplasia in a conditional mutant (B) compared with wild-type embryo (A) at E18.5. Asterisks indicate thymic lobes. (C-E) Intracardiac phenotype in wild-type (C), conditional (D) and *Tbx1*$^{–/–}$ (E) mutants. Embryos in D and E have essentially identical phenotypes. C′-E′ aortic arch and great artery patterning in wild-type (C′), conditional (D′) and *Tbx1*$^{–/–}$ (E′) mutants at E18.5. (F,G) Lateral views of ink-injected *Tbx1*$^{+/–}$ (F) and conditional mutant (G) embryos at E10.5. Note the absence of the 4th pharyngeal arch artery and reduced distance between the 3rd and 6th in the conditional mutant embryo. ao: aorta; rcc and lcc: right and left common carotid artery; rsa and lsa: right and left subclavian artery; pa: pulmonary arteries; pt: pulmonary trunk; RV: right ventricle; T: truncus arteriosus; VSD: ventricular septum defect. Scale bars: 1 mm in A-E and C′-E′; 200 μm in F,G.

Nkx2.5^{cre} induces recombination in a portion of the pharyngeal endoderm that expresses *Tbx1* in the 4th pouch, around the 4th arch, and 3rd pouch (Fig. 4G,H). These overlaps correlate well with small 4th arch and small thymus, which is derived from the 3rd pharyngeal pouches. The other structures of the pharyngeal apparatus were normal. Conditional mutants have no separation between the aorta and pulmonary trunk (Fig. 3D,D′), suggesting a defect of the AP septum. Normally, this structure forms around E10.5 from the dorsal wall of the aortic sac, between the confluence of the 4th and 6th PAAs, but it is absent in conditional mutants (Fig. 4I,J), suggesting a morphogenetic defect of the aortic sac. *Nkx2.5*^{cre}-induced recombination and *Tbx1* expression overlap in the endodermal lining of the aortic sac, providing a regional correlation with the morphogenetic defect (Fig. 4K,L). Alternatively, the AP septum abnormality could be secondary to reduced neural crest migration through the 4th arch. However, such reduction appears to be modest, and the AP septum is also contributed by neural crest cells of the 3rd and 6th pharyngeal arches (Phillips et al., 1987), which migrate normally in conditional mutants (arrows in Fig. 4C,D).

Conditional deletion of *Tbx1* reduces cell proliferation in the splanchnic mesoderm

Immunohistochemistry with an anti-α-sma antibody showed a thinner and discontinuous immunoreaction in the OFT myocardial layer of conditional mutants (Fig. 5A-C,A′-C′). The growth of the myocardial layer of the OFT relies mainly on cell migration from the SHF because cell proliferation activity is modest in the OFT, but it is high in the SHF. Thus, a possible explanation for reduced contribution of cells to the OFT is reduced proliferation in the SHF. We performed a BrdU assay in embryos with 32 and 29 somites, and results showed that the mitotic index in the SHF and adjacent splanchnic mesoderm of conditional mutants is reduced by 18% and 19%, respectively, compared with somite-matched wild-type embryos (Table 1). In contrast, we found no significant difference in the myocardial OFT and in tissues where there is no overlap between *Tbx1* expression and *Nkx2.5*^{Cre}-induced recombination (Table 1). This result is consistent with overlap between *Tbx1* expression and *Nkx2.5*^{Cre}-driven recombination in the SHF region (Fig. 6D,G).

Chimera analyses support a cell non-autonomous role of Tbx1 in the SHF

The Tbx1 role in cell proliferation could be produced through a cell-autonomous mechanism or through activation of an extracellular signaling system (cell non-autonomous mechanism). Our cell fate mapping data show that loss of function of Tbx1 causes overall reduction of cell contribution to the OFT, not restricted to *Tbx1*-traced cells, suggesting a cell non-autonomous mechanism. To further investigate this issue, we asked whether *Tbx1*$^{–/–}$ cells may have a proliferation disadvantage in populating the SHF when competing with wild-type cells, in a chimeric context. Therefore, we generated *Tbx1*$^{–/–}$:*Tbx1*$^{+/+}$ chimeric embryos as previously described (Vitelli et al., 2003). In this experimental approach, mutant cells that have a transcriptionally active (but non-functional) *Tbx1* gene will be blue upon X-gal staining, because they express a *lacZ* reporter gene inserted into the *Tbx1* locus. Results showed that *Tbx1*$^{–/–}$ blue cells are not excluded from the SHF of chimeras (n=10) and produce an X-gal staining pattern similar to the one observed in *Tbx1*$^{+/–}$:*Tbx1*$^{+/+}$ chimeras (n=8)

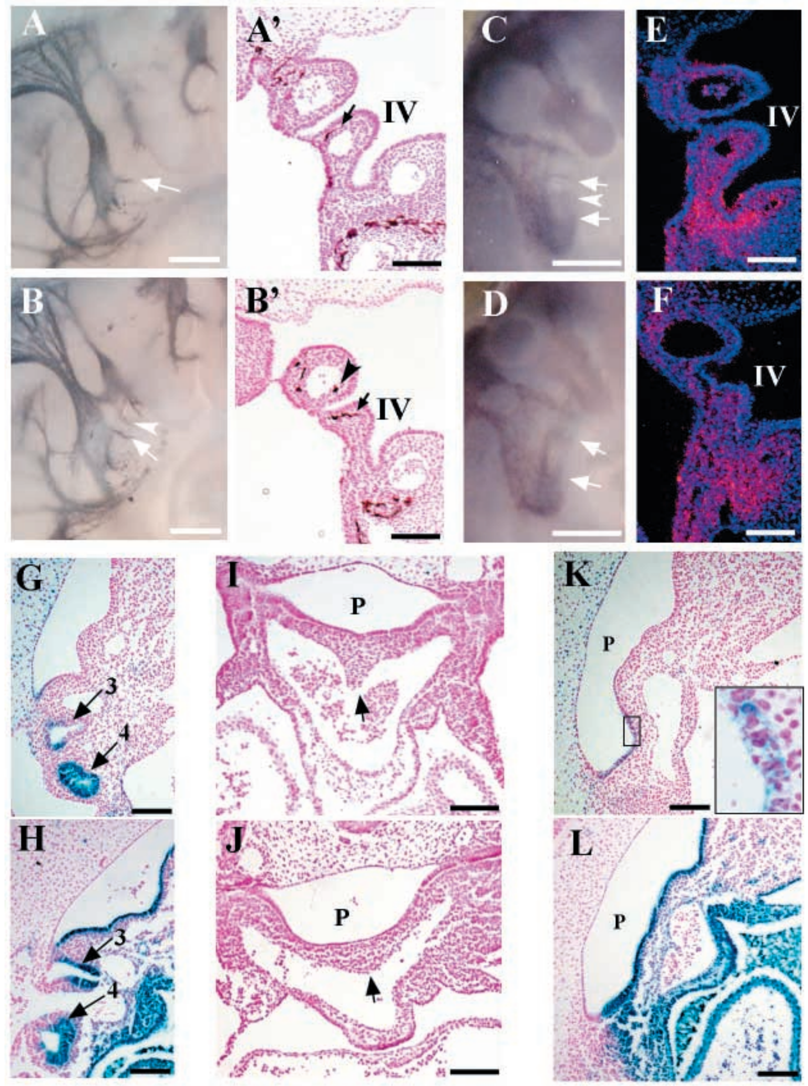

Fig. 4. Neural crest cell migration and AP septum phenotype in conditional mutants (E10-E10.5). (A-F) Fourth pharyngeal arch and neural crest migration phenotype in controls (*Tbx1*$^{flox/+}$) (A,A′,C,E) and conditional mutants (B,B′,D,F). (A,B) Lateral view of wholemount immunohistochemistry with an anti-neurofilament M antibody (dorsal is left), note the abnormal branch of the glossopharyngeal nerve bundle (arrowheads in B,B′). The 4th pharyngeal arch is small with an apparently normal vagus nerve (arrows) but absent 4th pharyngeal arch artery (A′,B′). A′ and B′ are coronal sections of the embryos shown in A and B, respectively. (C-D) Lateral view of wholemount RNA in situ hybridization with a neural crest marker (*CrabpI*) (dorsal is left), note the reduced staining at the 4th pharyngeal arch in the conditional mutant (compare with the region indicated by arrowhead in the wild-type embryo in C). (E,F) Radioactive in situ hybridization with the same probe on tissue sections of 32-somite embryos (E, wild type; F, conditional mutant). There is reduced expression of the neural crest marker and absence of the 4th PAA. (G,H) Partial overlap between *Tbx1* expression (visualized by the *Tbx1-lacZ* knock-in pattern) (G) and *Nkx2.5*^{cre}-induced recombination (visualized by the R26R reporter) (H) in the endoderm of the 3rd and 4th pharyngeal pouches (arrows), sagittal sections. (I,J) Coronal sections show absence of the AP septum (arrow) in a conditional mutant (J), compared with a control (*Nkx2.5*$^{Cre/+}$;*Tbx1*$^{+/-}$) embryo (I). (K,L) Sagittal sections, stained with X-gal, showing overlap between *Tbx1* expression (visualized by the *Tbx1-lacZ* knock-in pattern, K) and *Nkx2.5*^{Cre}-induced recombination (visualized by R26R reporter, L) in the endoderm lining the aortic sac adjacent to the AP septum (detail magnified in box, 5×). IV, fourth pharyngeal arch. P, pharynx. The developmental stages of embryos shown in G-L are in the range of 34-37 somites. Scale bars: 200 μm in A-D; 100 μm in the others.

Table 1. Results of BrdU assay in conditional mutants and somite-matched controls

Embryo (somites)	Tissue	Total cell number	BrdU +	Mitotic index
Control 1 (29)	Splanchnic mesoderm	1011	488	0.48
	OFT myocardium	1187	117	0.099
	Brain	1175	650	0.55
Conditional mutant 1 (29)	Splanchnic mesoderm	917	360	0.39 (*P*=0.00007)
	OFT myocardium	1232	107	0.087 (*P*=0.32)
	Brain	1142	640	0.56 (*P*=0.73)
Control 2 (32)	Splanchnic mesoderm	1377	652	0.47
	OFT myocardium	1198	116	0.097
	Somites	1065	618	0.58
Conditional mutant 2 (32)	Splanchnic mesoderm	785	306	0.39 (*P*=0.0001)
	OFT myocardium	1178	100	0.085 (*P*=0.31)
	Somites	1168	702	0.60 (*P*=0.32)

P values refer to comparison with respective controls, and are calculated with a χ-square test.

(Fig. 6A-B) and *lacZ* knock-in germ line mutants (Fig. 2K,K′). These results provide further support to the hypothesis that *Tbx1* is not required cell-autonomously for SHF cell proliferation.

Fgf10 is a direct target of Tbx1 in a tissue culture system

The above results suggest that Tbx1 may activate an extracellular signaling system that regulates cell proliferation

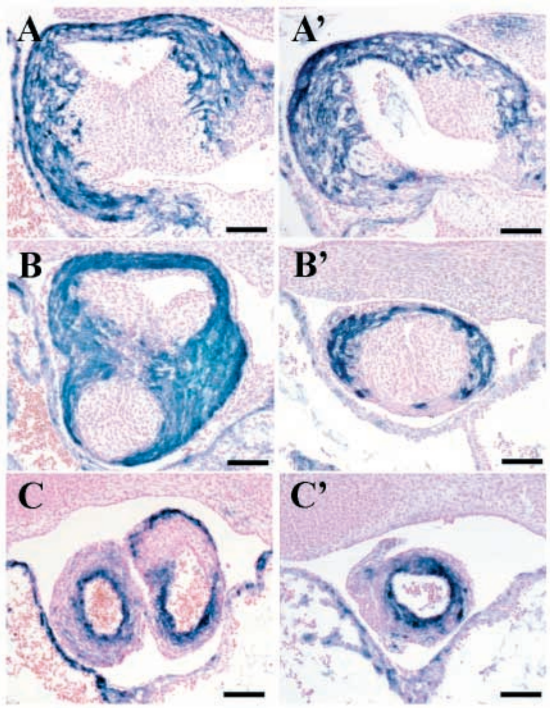

Fig. 5. Myocyte differentiation in OFT of conditional mutants. (A-C) Immunohistochemistry with an anti-α-smooth muscle actin antibody on coronal sections of E12.5 control (*Tbx1*$^{flox/–}$) (A-C) and conditional mutant (A′-C′) embryos at the level of the conus (A,A′), conal-truncal transition (B,B′) and truncus (C,C′). Note the reduced immunoreactivity in conditional mutants (A′-C′), especially at the conal-truncal transition. Scale bars: 100 μm.

in the SHF. To date, no transcriptional target of Tbx1 has been reported, but it has been shown that *Fgf10* expression is reduced in the SHF of *Tbx1*$^{–/–}$ mutants, by in situ hybridization (Kochilas et al., 2002; Vitelli et al., 2002c). It has been shown that FGF signaling can induce cell proliferation in SHF explants (Waldo et al., 2001), so Fgf10 might mediate, at least in part, a cell non-autonomous function of Tbx1 in this region. Recently, it has been shown that *Tbx5* can activate *Fgf10* through a conserved T-box binding element (TBE) located in the 5′ region of the *Fgf10* gene (Agarwal et al., 2003). Therefore, we asked whether Tbx1 could also activate the *Fgf10* gene via this TBE. To this end, we co-transfected into COS-7 cells a *Tbx1* expression vector and an *Fgf10* promoter-luciferase construct. We observed up to 20-fold activation of luciferase activity in repeated experiments, but when we co-transfected the *Tbx1* expression vector with an *Fgf10* promoter construct carrying a mutant TBE (Agarwal et al., 2003), we observed no activation (Fig. 6C), demonstrating that this binding site is required for activation. For comparison, the same experiment was performed with a *Tbx5* expression vector with similar results, raising the intriguing possibility that different T-box transcription factors may share target genes. In situ hybridization on tissue sections of wild-type embryos showed overlap between *Tbx1* and *Fgf10* expression in the SHF region (Fig. 6D,E). In addition, *Fgf10* expression in this region is reduced or abolished in conditional mutants (Fig. 6F), consistent with overlap with *Nkx2.5*^{Cre}-driven recombination (Fig. 6G). These results identify Fgf10 as a candidate mediator of the Tbx1 cell non-autonomous role in cell proliferation in the SHF.

Discussion

Del22q11 causes a broad range of phenotypic abnormalities, many related to developmental defects of the pharyngeal apparatus. Mouse studies have attributed these abnormalities to haploinsufficiency of *Tbx1*, a T-box transcription factor, included in the *del22q11* region. Recently, mutational analyses have found *TBX1* gene mutations in patients with a ‘pharyngeal’ phenotype essentially identical to that associated with *del22q11* (Yagi et al., 2003), demonstrating that *Tbx1* has similar developmental roles in human and mouse. A cardinal feature of *del22q11*/DGS is congenital heart disease, which includes aortic arch/great artery patterning defects and OFT defects. *Tbx1*$^{+/–}$ mice have mainly aortic arch patterning defects, whereas *Tbx1*$^{–/–}$ embryos have severe OFT abnormalities, but they also have severe developmental defects of the entire pharyngeal apparatus. In this study we asked whether the OFT phenotype in *Tbx1*$^{–/–}$ embryos is merely a consequence of pharyngeal apparatus abnormalities, and, if not, what are the specific roles of *Tbx1* in OFT morphogenesis.

Tbx1 has direct roles in OFT morphogenesis

Our data show that *Tbx1*$^{neo/neo}$ animals present with severe abnormalities of the pharyngeal apparatus, including loss of the 3rd-6th pairs of pharyngeal arches and arteries, as in *Tbx1*$^{–/–}$ embryos. However, the OFT phenotype is milder in approximately half of the *Tbx1*$^{neo/neo}$ embryos. Thus, the OFT mutant phenotype is partially independent of the pharyngeal phenotype. Conversely, *Nkx2*.5^{cre}-induced somatic deletion of *Tbx1* recapitulates the OFT phenotype of *Tbx1*$^{–/–}$ animals, even though the abnormalities of the pharyngeal apparatus are much milder. Overall, these data clearly indicate that Tbx1 has specific functions in OFT morphogenesis.

Tbx1 regulates cell contribution to the OFT

Tbx1 is expressed in progenitors as well as in differentiated, resident myocytes and endothelial cells of the OFT. However, our conditional deletion experiments indicate that Tbx1 function is not required in myocardial or endothelial cells. Instead, cell fate mapping experiments indicate that *Tbx1* regulates, but is not required for contribution of myocytes, and possibly other cell types, to the OFT. Most probably, Tbx1 does not directly regulate cell proliferation of progenitor cells because in chimeras, *Tbx1*$^{–/–}$ cells do not have a proliferative disadvantage in the SHF. Thus, the Tbx1 role in regulating cell contribution to the OFT will probably be cell non-autonomous. Fgf10 is a candidate mediator of this function because its expression in the SHF is abolished in *Tbx1*$^{–/–}$, *Tbx1*$^{neo/neo}$, and conditional mutants, and Tbx1 can directly activate the *Fgf10* promoter in a tissue culture assay. Interestingly though, *Fgf10*$^{–/–}$ animals do not have OFT defects, raising the question as to whether Tbx1 also activates other *Fgf* genes or other extracellular signaling systems critical for OFT morphogenesis. Alternatively, *Fgf10*$^{–/–}$ animals may not have OFT defects because other *Fgf* genes compensate for the loss of *Fgf10*, as proposed recently (Kelly and Buckingham, 2002).

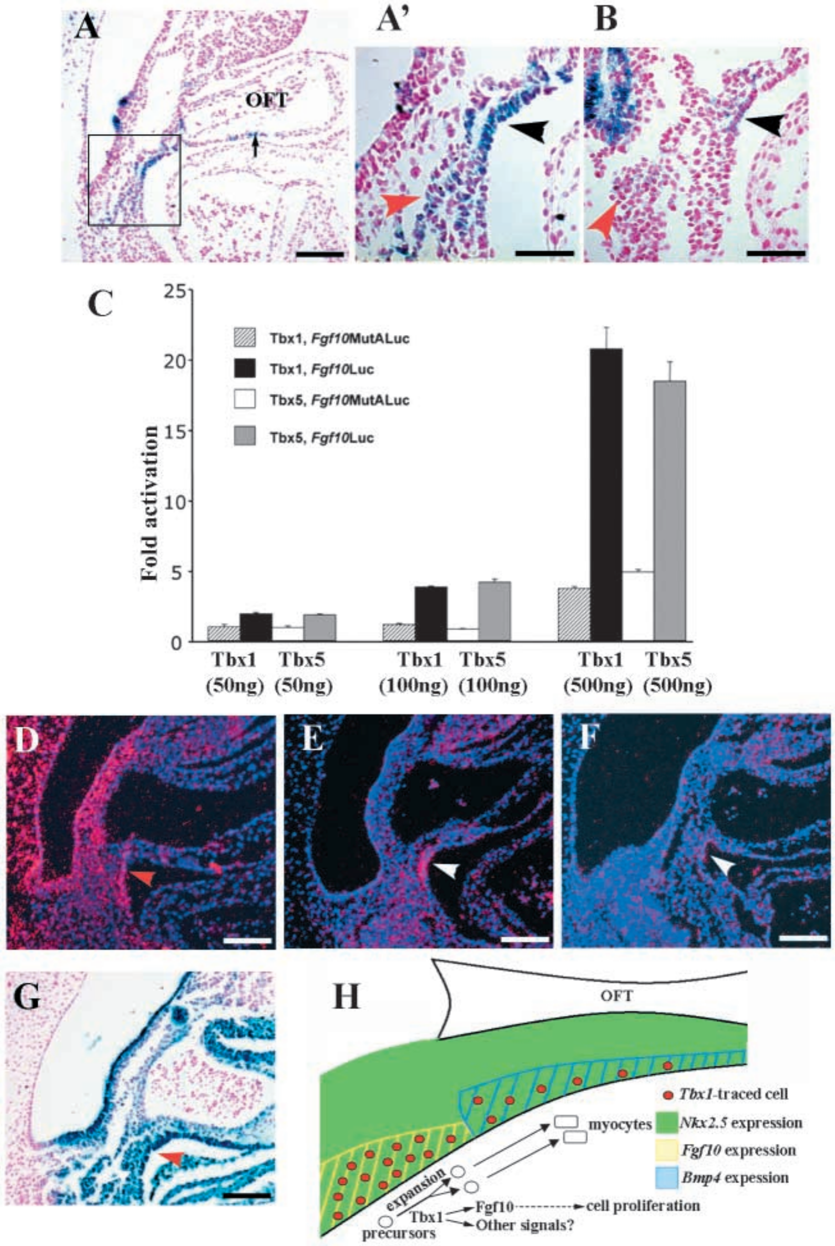

Fig. 6. Chimera analysis and *Fgf10* regulation by Tbx1. (A-B) Contribution of *Tbx1*$^{-/-}$ cells to OFT (arrow) and SHF (square box magnified in A′) in a chimeric E10.5 embryo, compared with the same region of a *Tbx1*$^{+/-}$ chimera. Note that *Tbx1*$^{-/-}$ cells appear more intensely stained because they carry two *lacZ* knock-in alleles. (C) Tbx1 and Tbx5 activate the *Fgf10* promoter carrying a wild-type (*Fgf10Luc*) but not mutant (*Fgf10MutAluc*) T-box binding element. Scale bars: 100 μm in A; 50 μm in A′ and B. (D-F) RNA in situ hybridization on sagittal sections (E10.25) of control embryos (*Tbx1*$^{flox/+}$) showing overlap of *Tbx1* expression (D) and *Fgf10* expression (E) in the SHF region (arrowheads). *Fgf10* expression is reduced or absent in a conditional mutant (F). (G) Sagittal section (at the same stage) of an *Nkx2.5*$^{Cre/+}$;R26R embryo showing extensive recombination that includes the region in which *Tbx1* is expressed. (H) Schematic drawing of the proposed model for *Tbx1* function in the SHF. Scale bars: 100 μm in D-G.

Tbx1 has at least two roles in OFT morphogenesis

Consistent with previously discussed data, the OFT of *Tbx1* conditional mutants have reduced numbers of α-sma-positive cells. This correlates well with a significant downregulation of cell proliferation in the SHF. In contrast, the proliferation of cells of the myocardial layer of the OFT is not affected in these mutants. Hence, the most probable explanation for the lower number of α-sma-positive cells in the OFT is a reduced supply from a pool of precursors, secondary to reduced cell proliferation. It is also possible that Tbx1 is required to specify a subpopulation of OFT myocyte precursors because the α-sma phenotype is more obvious in the region where truncal valve septation is occurring (Fig. 5B,B′). This is an intriguing observation because this cell population may have a specialized, patterning role in truncal valve septation. Interestingly, the *Drosophila* homologue of *Tbx1*, *Org-1*, is expressed in a subpopulation of visceral muscle cell precursors, the so-called pioneer cells, which have patterning activity (Lee et al., 2003).

Our data show that Tbx1 has an additional role in OFT morphogenesis because it is required for the formation of the AP septum in *Tbx1*$^{-/-}$, *Tbx1*$^{neo/neo}$, and conditional mutants. Because the AP septum is mainly contributed by neural crest-derived cells, it is possible that this phenotype is caused, at least in part, by the observed reduced population of migrating neural crest-derived cells in the 4th pharyngeal arch of conditional mutants. However, this reduction appears modest, and the conotruncal ridges, which are also populated by a substantial number of neural crest cells, are only slightly reduced in size. Therefore, we hypothesize that AP septum aplasia in conditional mutants is because of defective morphogenesis of the aortic sac. This morphogenetic defect is consistent with the pharyngeal segmentation defect observed in *Tbx1*$^{-/-}$ mutants. It has been proposed that the *Tbx1* role in pharyngeal segmentation may be related to its expression in the pharyngeal endoderm (Baldini, 2002; Lindsay, 2001). The AP septum phenotype in conditional mutants correlates well with overlap of *Tbx1* and *Nkx2.5*^{Cre}-induced recombination in the pharyngeal endoderm and wall of the aortic sac.

SHF function and congenital heart disease

Presumably, an as yet unknown signal induces naïve splanchnic mesodermal cells to an OFT myocardial fate. One of the consequences of this signal is the expression of *Nkx2.5*, possibly one of the first markers of specification of this cell population. Nkx2.5 is required for the formation of a canalized OFT conduit (Lyons et al., 1995; Tanaka et al., 1999) (M.M., unpublished). However, proper morphogenesis of the OFT requires sustained contribution of specified cells throughout an extended period of time (approximately between E9.0 and E11.0) because resident OFT myocytes have a low proliferative capacity at this stage. We propose that the function of Tbx1 is to maintain cell contribution to the OFT at a sufficiently high level to support growth and remodeling of the OFT (Fig. 6H). This function may be directed towards the entire population of myocyte precursors, or perhaps more probable, towards a specific sub-population. Whatever the target cell population may be, the effect of *Tbx1* on cell proliferation is cell non-autonomous.

Our data provide the first evidence that a genetic defect related to human congenital heart disease affects directly the function of the SHF. Our data do not allow us to determine exactly what type of defect is caused by SHF malfunction. However, on the basis of our observations it is reasonable to speculate that these may include defects of OFT alignment (also consistent with results obtained in chick) (Yelbuz et al., 2002) and defects of truncal valve septation. Thus, many of the common heart defects observed in children, including Tetralogy of Fallot, double outlet right ventricle, some types of ventricular septal defects and some types of truncus arteriosus, may be caused by SHF malfunction. Therefore, it is very probable that the definition of genetic pathways regulating SHF function will lead to other genes involved in congenital heart disease. The identification of the role of Tbx1 in the SHF is the first step in this direction.

We wish to thank M. Reese, H. Sobotka, P. Terrell and C. Sparks for valuable technical assistance, P. Soriano, M. Yangisawa and M. Schneider for mouse lines, A. Bradley for the AB2.2 embryonic stem cell line, M. Reth for the MerCreMer construct, F. Cerrato for help with the analysis of *Tbx1*$^{neo/neo}$ heart morphology, and F. Vitelli and J. Martin for critical reading of the manuscript. This work was funded by grants HL51524, HL64832, HL67155 and DE14521 from the National Institutes of Health (A.B.), and grant #0255829Y from the AHA Texas Affiliate (E.A.L.). We also acknowledge the support of the Baylor Mental Retardation Research Center Transgenic Core. B.G.B. is supported by grants from the Canadian Institutes of Health Research, The Heart and Stroke Foundation of Ontario and the March of Dimes Birth Defects Foundation, and holds a Canada Research Chair in Developmental Cardiology.

References

Agah, R., Frenkel, P. A., French, B. A., Michael, L. H., Overbeek, P. A. and Schneider, M. D. (1997). Gene recombination in postmitotic cells. Targeted expression of Cre recombinase provokes cardiac-restricted, site-specific rearrangement in adult ventricular muscle in vivo. *J. Clin. Invest.* **100**, 169-179.

Agarwal, P., Wylie, J. N., Galceran, J., Arkhitko, O., Li, C., Deng, C., Grosschedl, R. and Bruneau, B. G. (2003). Tbx5 is essential for forelimb bud initiation following patterning of the limb field in the mouse embryo. *Development* **130**, 623-633.

Albrecht, U., Eichele, G., Helms, J. A. and Lu, H. C. (1997). Visualization of gene expression patterns by in situ hybridization. In *Molecular and Cellular Methods in Developmental Toxicology* (ed. G. P. Daston), pp. 23-48. New York: CRC Press, Inc.

Baldini, A. (2002). DiGeorge syndrome: the use of model organisms to dissect complex genetics. *Hum. Mol. Genet.* **11**, 2363-2369.

Biben, C., Weber, R., Kesteven, S., Stanley, E., McDonald, L., Elliott, D. A., Barnett, L., Koentgen, F., Robb, L., Feneley, M. et al. (2000). Cardiac septal and valvular dysmorphogenesis in mice heterozygous for mutations in the homeobox gene Nkx2-5. *Circ. Res.* **87**, 888-895.

Bruneau, B. G., Nemer, G., Schmitt, J. P., Charron, F., Robitaille, L., Caron, S., Conner, D. A., Gessler, M., Nemer, M., Seidman, C. E. et al. (2001). A murine model of Holt-Oram syndrome defines roles of the T-box transcription factor Tbx5 in cardiogenesis and disease. *Cell* **106**, 709-721.

Chapman, D. L., Garvey, N., Hancock, S., Alexiou, M., Agulnik, S. I., Gibson-Brown, J. J., Cebra-Thomas, J., Bollag, R. J., Silver, L. M. and Papaioannou, V. E. (1996). Expression of the T-box family genes, Tbx1-Tbx5, during early mouse development. *Dev. Dyn.* **206**, 379-390.

Giguere, V., Lyn, S., Yip, P., Siu, C. H. and Amin, S. (1990). Molecular cloning of cDNA encoding a second cellular retinoic acid- binding protein. *Proc. Natl. Acad. Sci. USA* **87**, 6233-6237.

Hayashi, S. and McMahon, A. P. (2002). Efficient recombination in diverse tissues by a tamoxifen-inducible form of Cre: a tool for temporally regulated gene activation/inactivation in the mouse. *Dev. Biol.* **244**, 305-318.

Jerome, L. A. and Papaioannou, V. E. (2001). DiGeorge syndrome phenotype in mice mutant for the T-box gene, *Tbx1*. *Nat. Genet.* **27**, 286-291.

Jiang, X., Rowitch, D. H., Soriano, P., McMahon, A. P. and Sucov, H. M. (2000). Fate of the mammalian cardiac neural crest. *Development* **127**, 1607-1616.

Kelly, R. G. and Buckingham, M. E. (2002). The anterior heart-forming field: voyage to the arterial pole of the heart. *Trends Genet.* **18**, 210-216.

Kelly, R. G., Brown, N. A. and Buckingham, M. E. (2001). The arterial pole of the mouse heart forms from Fgf10-expressing cells in pharyngeal mesoderm. *Dev. Cell* **1**, 435-440.

Kirby, M. L. and Waldo, K. L. (1995). Neural crest and cardiovascular patterning. *Circ. Res.* **77**, 211-215.

Kisanuki, Y. Y., Hammer, R. E., Miyazaki, J., Williams, S. C., Richardson, J. A. and Yanagisawa, M. (2001). Tie2-Cre transgenic mice: a new model for endothelial cell-lineage analysis in vivo. *Dev. Biol.* **230**, 230-242.

Kochilas, L., Merscher-Gomez, S., Lu, M. M., Potluri, V., Liao, J., Kucherlapati, R., Morrow, B. and Epstein, J. A. (2002). The role of neural crest during cardiac development in a mouse model of DiGeorge syndrome. *Dev. Biol.* **251**, 157-166.

Lee, H. H., Norris, A., Weiss, J. B. and Frasch, M. (2003). Jelly belly protein activates the receptor tyrosine kinase Alk to specify visceral muscle pioneers. *Nature* **425**, 507-512.

Li, J., Chen, F. and Epstein, J. A. (2000). Neural crest expression of Cre recombinase directed by the proximal Pax3 promoter in transgenic mice. *Genesis* **26**, 162-164.

Lindsay, E. A. (2001). Chromosomal microdeletions: dissecting del22q11 syndrome. *Nat. Rev. Genet.* **2**, 858-868.

Lindsay, E. A., Botta, A., Jurecic, V., Carattini-Rivera, S., Cheah, Y.-C., Rosenblatt, H. M., Bradley, A. and Baldini, A. (1999). Congenital heart disease in mice deficient for the DiGeorge syndrome region. *Nature* **401**, 379-383.

Lindsay, E. A., Vitelli, F., Su, H., Morishima, M., Huynh, T., Pramparo, T., Jurecic, V., Ogunrinu, G., Sutherland, H. F., Scambler, P. J. et al. (2001). Tbx1 haploinsufficieny in the DiGeorge syndrome region causes aortic arch defects in mice. *Nature* **410**, 97-101.

Lyons, I., Parsons, L. M., Hartley, L., Li, R., Andrews, J. E., Robb, L. and Harvey, R. P. (1995). Myogenic and morphogenetic defects in the heart tubes of murine embryos lacking the homeobox gene Nkx2-5. *Genes Dev.* **9**, 1654-1666.

Merscher, S., Funke, B., Epstein, J. A., Heyer, J., Puech, A., Min Lu, M. M., Xavier, R. J., Demay, M. B., Russell, R. G., Factor, S. et al. (2001). TBX1 is responsible for cardiovascular defects in Velo-Cardio-Facial/DiGeorge syndrome. *Cell* **104**, 619-629.

Mjaatvedt, C. H., Nakaoka, T., Moreno-Rodriguez, R., Norris, R. A., Kern, M. J., Eisenberg, C. A., Turner, D. and Markwald, R. R. (2001). The outflow tract of the heart is recruited from a novel heart-forming field. *Dev. Biol.* **238**, 97-109.

Moses, K. A., DeMayo, F., Braun, R. M., Reecy, J. L. and Schwartz, R. J. (2001). Embryonic expression of an Nkx2-5/Cre gene using ROSA26 reporter mice. *Genesis* **31**, 176-180.

Phillips, M. T., Kirby, M. L. and Forbes, G. (1987). Analysis of cranial neural crest distribution in the developing heart using quail-chick chimeras. *Circ. Res.* **60**, 27-30.

Sohal, D. S., Nghiem, M., Crackower, M. A., Witt, S. A., Kimball, T. R., Tymitz, K. M., Penninger, J. M. and Molkentin, J. D. (2001). Temporally regulated and tissue-specific gene manipulations in the adult and embryonic heart using a tamoxifen-inducible Cre protein. *Circ. Res.* **89**, 20-25.

Soriano, P. (1999). Generalized *lacZ* expression with the ROSA26 Cre reporter strain [letter]. *Nat. Genet.* **21**, 70-71.

Tanaka, M., Chen, Z., Bartunkova, S., Yamasaki, N. and Izumo, S. (1999). The cardiac homeobox gene Csx/Nkx2.5 lies genetically upstream of multiple genes essential for heart development. *Development* **126**, 1269-1280.

van den Hoff, M. J., Moorman, A. F., Ruijter, J. M., Lamers, W. H., Bennington, R. W., Markwald, R. R. and Wessels, A. (1999). Myocardialization of the cardiac outflow tract. *Dev. Biol.* **212**, 477-490.

Verrou, C., Zhang, Y., Zurn, C., Schamel, W. W. and Reth, M. (1999).

Comparison of the tamoxifen regulated chimeric Cre recombinases MerCreMer and CreMer. *Biol. Chem.* **380**, 1435-1438.

Vitelli, F., Lindsay, E. A. and Baldini, A. (2002a). Genetic dissection of the DiGeorge syndrome phenotype. *Cold Spring Harbor Symp. Quant. Biol.* **LXVII**, 327-332.

Vitelli, F., Morishima, M., Taddei, I., Lindsay, E. A. and Baldini, A. (2002b). Tbx1 mutation causes multiple cardiovascular defects and disrupts neural crest and cranial nerve migratory pathways. *Hum. Mol. Genet.* **11**, 915-922.

Vitelli, F., Taddei, I., Morishima, M., Meyers, E. N., Lindsay, E. A. and Baldini, A. (2002c). A genetic link between Tbx1 and fibroblast growth factor signaling. *Development* **129**, 4605-4611.

Vitelli, F., Viola, A., Morishima, M., Pramparo, T., Baldini, A. and Lindsay, E. (2003). TBX1 is required for inner ear morphogenesis. *Hum. Mol. Genet.* **12**, 2041-2048.

Waldo, K. L., Kumiski, D. H., Wallis, K. T., Stadt, H. A., Hutson, M. R., Platt, D. H. and Kirby, M. L. (2001). Conotruncal myocardium arises from a secondary heart field. *Development* **128**, 3179-3188.

Yagi, H., Furutani, Y., Hamada, H., Sasaki, T., Asakawa, S., Minoshima, S., Ichida, F., Joo, K., Kimura, M., Imamura, S.-i. et al. (2003). Role of TBX1 in human del22q11.2 syndrome. *Lancet* **362**, 1366-1373.

Yelbuz, T. M., Waldo, K. L., Kumiski, D. H., Stadt, H. A., Wolfe, R. R., Leatherbury, L. and Kirby, M. L. (2002). Shortened outflow tract leads to altered cardiac looping after neural crest ablation. *Circulation* **106**, 504-510.